LOGO _____

Sub-GHz In-Body to Out-of-Body Communication Channel Modeling for Ruminant Animals for Smart Animal Agriculture

Arunashish Datta, Upinder Kaur, Victor Malacco, Mayukh Nath, Baibhab Chatterjee, Shawn S. Donkin, Richard M. Voyles and Shreyas Sen

Abstract—Sensors in and around the environment becoming ubiquitous has ushered in the concept of smart animal agriculture which has the potential to greatly improve animal health and productivity using the concepts of remote health monitoring which is a necessity in times when there is a great demand for animal products. The data from in and around animals gathered from sensors dwelling in animal agriculture settings have made farms a part of the Internet of Things space. This has led to active research in developing efficient communication methodologies for farm networks. This study focuses on the first hop of any such farm network where the data from inside the body of the animals is to be communicated to a node dwelling outside the body of the animal. In this paper, we use novel experimental methods to calculate the channel loss of signal at sub-GHz frequencies of 100 - 900 MHz to characterize the in-body to out-of-body communication channel in large animals. A first-of-its-kind 3D bovine modeling is done with computer vision techniques for detailed morphological features of the animal body is used to perform Finite Element Method based Electromagnetic simulations. The results of the simulations are experimentally validated to come up with a complete channel modeling methodology for in-body to out-of-body animal body communication. The experimentally validated 3D bovine model is made available publicly on GitHub. The results illustrate that an in-body to out-of-body communication channel is realizable from the rumen to the collar of ruminants with $\leq 90 dB$ path loss at sub-GHz frequencies (100 - 900MHz) making communication feasible. The developed methodology has been illustrated for ruminants but can also be used for other related in-body to out-of-body studies. Using the developed channel modeling technique, an efficient communication architecture can be formed for in-body to out-of-body communication in animals which paves the way for the design and development of future smart animal agriculture systems.

Index Terms—Remote health monitoring, Smart Animal Agriculture, Finite Element Method (FEM), Ruminant, In-Body to Out-of-Body Communication, Communication Channel Modeling, Animal Body Communication

I. INTRODUCTION

The ever-increasing demand for animal products has prompted studies on the use of innovative technology to enhance animal health and productivity. Real-time continuous health monitoring has been a topic of active research and development due to the potential to greatly improve the welfare and productivity of dairy animals. This has brought about the age of smart animal agriculture where data of various essential parameters affecting animal health and productivity is gathered and monitored in real-time. This has enabled animal agriculture to be a part of the Internet of Things and more specifically the Internet of Bodies (IoB) [1]-[3] with a network of sensors dwelling inside animals as well as their surroundings. This complex network requires means of efficient and low power communication of data around the farm. One such example of a farm network is illustrated in Fig. 1. The most critical and challenging part of this communication network to design is the first hop where the data from inside the animal's body is communicated to a node outside the body. Data collection from inside the animal body to be communicated outside the body brings multiple challenges. The

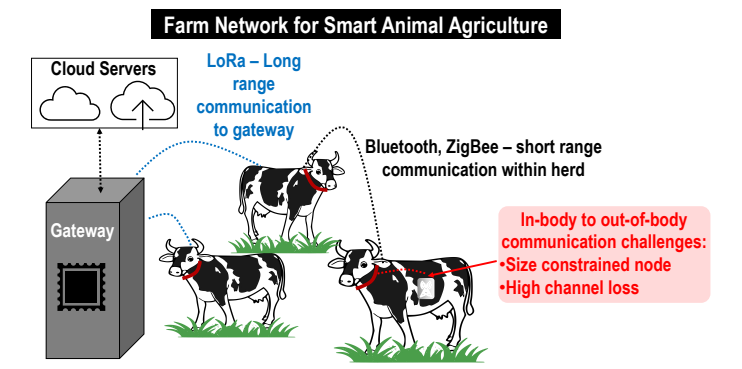


Fig. 1: An illustration of a farm network with different communication protocols working in tandem for an efficient communication architecture. The requirement and challenges in an in-body to out-of-body communication in animals is shown.

transmitter node being inside the body is size constrained and thus requires an energy efficient means of communication to increase the battery life of the device. Further, the communication channel consists of lossy body tissues resulting in a demand for higher transmit power which further results in quicker battery depletion. Thus, an in-body to out-of-body (IBOB) communication channel modeling is of paramount importance to come up with an efficient communication system. This study proposes a communication channel modeling and a novel first-of-its-kind open-source 3D bovine model for an animal body communication channel which is essential in the design of the communication system. The 3D bovine model is available publicly on GitHub [4].

In ruminants like bovines, rumen health is closely linked to the health of the animal and its eventual productivity. The rumen is populated with microorganisms that assist in its metabolic functioning. Thus, the rumen provides biomarkers that assist in the early detection of diseases like sub-acute ruminal acidosis (SARA). Thus, sensors monitoring rumen health are an essential part of the sensor network system described in Fig. 1. The challenges in communicating data from these sensors out of the body have prompted various studies. However, most of these studies have tried to communicate the data outside the body in an ad hoc manner without a detailed analysis of the communication channel that is being dealt with. Our work introduces a framework for performing a detailed analysis of any such animal body communication dealing with an in-body to out-of-body communication channel using experimental results and combining the data gathered to gain further insights using the developed model.

We perform experiments on a cannulated cow which allows access to the rumen of the animal at various sub-GHz frequencies over various critical positions on the body of the cow. The frequency range investigated in this paper of 100-900 MHz consists of important radio frequency bands like MedRadio [5], LoRa [6] and ZigBee [7]. The channel loss data gathered provides a measure of the expected values which is then used to validate the simulations. The morphological

features of the body of the cow are then captured using computer vision techniques to generate an accurate 3D model of the animal. This 3D model is then modified by adding layers emulating the tissues inside the cow's body which forms the complete simulation model. The model developed is used to perform Finite Element Method (FEM) based electromagnetic field analysis to generate channel loss values which are compared with the experimental data. This whole procedure is described pictorially in Fig. 2.

The key contributions of this paper are as follows:

- Detailed experiments for in-body to out-of-body communication on a cannulated cow performed around the complete range of sub-GHz frequencies.
- Using computer vision techniques to generate a 3D animal model accurately modeling the morphological features of the animal that the experiments were carried out on.
- Updating the generated 3D model of the cow to make it realistic by adding layers emulating tissue properties of the animal body.
- Performing detailed simulations controlling the various parameters affecting the channel loss characteristics like position and orientation of the transmitter and receiver across the sub-GHz range of frequencies.
- A first-of-its-kind method of communication channel modeling for in-body to out-of-body communication for bovines. This method of experimentally verified channel modeling can be replicated across other similar scenarios involving in-body to out-of-body communication in animals. The 3D bovine model developed is made available publicly [4] for further research involving FEM simulations for farm environments.

The subsequent sections are organized as follows: Section II provides an overview of related work that has been performed in the domain of in-body to out-of-body communication and channel modeling for bovines. In section III, we perform an in-depth study of the experimental setup and the results obtained from the experiments. Section IV details the development of the novel 3D bovine model and compares the results obtained from the simulations with the experiments to validate the model. In section V, a detailed discussion of the use cases for the novel model developed and our future work is performed. Section VI summarizes our findings and provides our concluding thoughts on this study.

II. RELATED WORK

In this study, we analyze the in-body to out-of-body communication channel for an animal body communication system using detailed experiments and Finite Element Method (FEM) based simulations. Previous studies have attempted similar in-body to out-of-body channel modeling based on FEM based electromagnetic simulations for human body [8]. However, complex human body models with detailed tissue properties have been available in literature [9]. However, such detailed 3D models accurately defining the features of bovines have not been previously used for FEM based EM analysis.

Attempts at channel modeling for animals have previously been made with a simplified simulation model [10], [11] with layers of tissues to approximate the channel loss due to the tissue properties or use animal phantoms to emulate the tissue properties [12], [13]. However, these simulations don't accurately model the features of the animal body thus making it impossible to gauge the effect of the position and orientation of the transmitting or receiving device. Further, such simulation models provide a very simplified view of the animal body and are inefficient in modeling the effects of the transmitter being inside the body of the animal with acceptable accuracy.

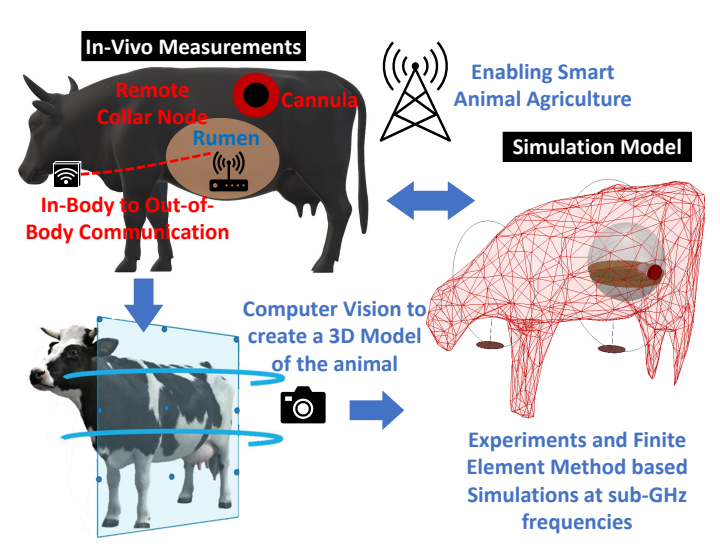


Fig. 2: An overview of the method used for channel modeling for in-body to out-of-body communication in ruminant animals is illustrated. Experiments on a cannulated cow is performed and the results are used to validate the FEM based EM simulations on the 3D bovine model developed using computer vision techniques which is made available publicly on GitHub.

This study is an extension of the work done by Datta et al. [14], where a simpler simulation model was used to perform FEM based simulations. The simulation model used in the previous study doesn't model the ruminal space with a great deal of accuracy. Further, the channel model developed is at a specific frequency of 400 MHz. This study provides a complete view of the effect that the transmitter and receiver system used has on the communication channel model and channel loss at different frequencies across the sub-GHz spectrum. We further analyze the channel loss characteristics at various frequencies, positions and orientations of the communication system and compare it with the loss that a typical commercial transceiver system can handle to figure out the best region of operation for efficient in-body to out-of-body communication.

III. EXPERIMENTAL VALIDATION

A. Goal of Experiments

The in-body to out-of-body animal body communication system is studied to analyze the channel loss experimentally. The huge mass of attenuating body tissues results in a high channel loss. The aim in these experiments is to analyze this channel loss at various critical positions on the bovine. This analysis will allow us to ascertain if a typical commercial transceiver with a transmit power of 0 dBm with a receiver sensitivity of -90 dBm can be used to perform in-body to out-of-body communication in a bovine efficiently at sub-GHz frequencies. Thus, our channel loss response is measured and a reference path loss of 90 dB is used to comment on whether the system is suitable to be used at a particular frequency with a commercial transceiver system.

B. Experimental Setup

The experiments were performed at the Purdue Dairy Farm to analyze the channel loss response at sub-GHz frequencies. The experiments were approved by the Purdue Institutional Animal Care and Use Committee (IACUC). The experiments have been performed in-situ on a cannulated cow as shown in Fig. 3 over multiple days and the aggregate values are presented. The breed of cow used for our

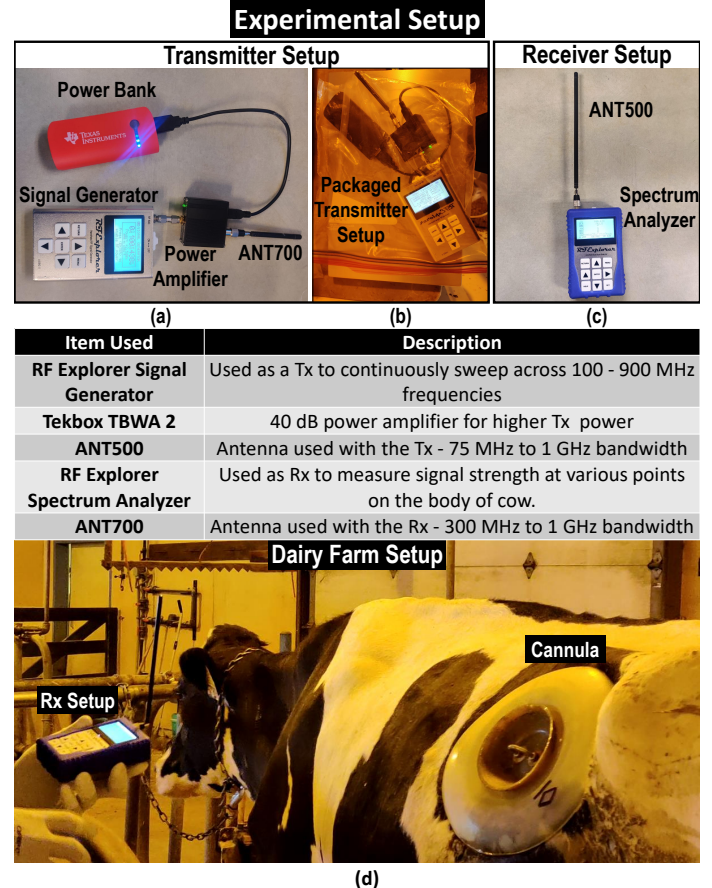


Fig. 3: (a) The transmitter setup used for experiments is shown. A handheld signal generator is used with a broadband 40 dB power amplifier (Tekbox TBWA 2) and a telescopic antenna (ANT700). (b) The transmitter is packaged inside multiple ziplock bags keeping the setup airtight. (c) The receiver setup consists of a handheld spectrum analyzer with another telescopic antenna (ANT500). The complete setup used for the experiments is described in the subsequent table. (d) Experiments are conducted on a cannulated cow in a dairy farm.

experiments were female Holstein heifers. The transmitter setup is completely placed inside the rumen and the receiver is positioned at various points close to the body of the cow where an actual receiver is typically present. It is essential that the transmitter setup is completely inside the rumen because if the transmitter is connected with an SMA to be programmed from outside the cow's body, the leakage from the SMA cables will result in inaccurate values of path loss as has been observed in our initial experiments.

The transmitter (Fig. 3 (a)) consists of a handheld RF Explorer Signal Generator which is programmed to automatically sweep across the frequencies from 100 MHz to 900MHz with 9 points on the decade. We use a high gain (40dB) power amplifier (Tekbox TBWA2) and an ANT700 antenna [15]. The power amplifier is essential for accurate path loss readings as a low transmit power will result in the low signal strength on the receiver side thus decreasing the accuracy of the readings when signal strength is close to the limits defined by the receiver sensitivity. The transmit power of the setup across all the frequencies lies between 15-16 dBm. The transmitter is placed inside the rumen through the cannula packaged inside an airtight casing as illustrated in Fig. 3 (b). The receiver setup (Fig. 3 (c)) consists of a handheld RF Explorer Spectrum Analyzer with an ANT500 antenna to pick up the signal strength at the transmitted frequencies. The

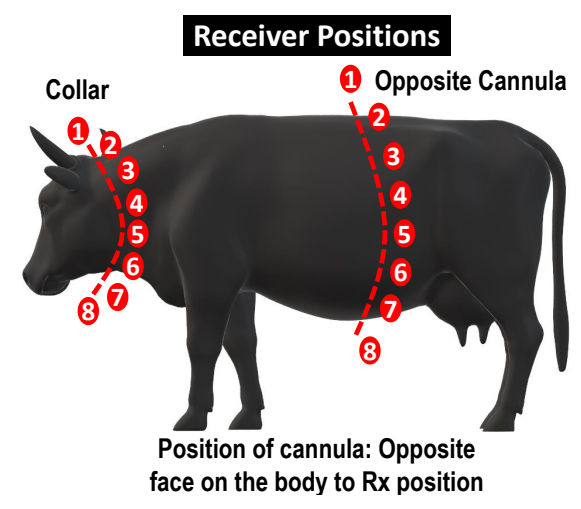


Fig. 4: The receiver in this study is placed in identified critical positions that have been shown in this figure. The two important positions for the receiver identified are 1) around the collar which is the most accessible, 2) on the body near the cannula where the channel loss is the least due to small communication channel.

complete dairy farm setup is illustrated in Fig. 3 (d).

The two critical positions of the receiver as illustrated in Fig. 4 have been identified as (a) Collar of the cow, which has been previously used [16] as a position where transceiver nodes are placed due to its accessibility and (b) On the body of the cow opposite to where the cannula is placed due to the lowest channel loss present in that region as the channel length is smaller and thus the body tissues present between the transmitter and receiver is lesser than other regions on the body. The receiver is moved along the two positions defined in Fig. 4 to calculate the worst case channel loss in such a configuration of the transmitting and receiving devices. To get the highest channel loss, the receiver is moved along 8 points of the two identified locations on the opposite side of the cannula where the path loss is higher (Fig. 13) than the path loss on the side of the cannula. This is due to lesser body tissues present to attenuate the signal on the side of the cannula.

C. Discussion: Rumen and Position of Transmitter

The rumen is a dynamic environment with particles inside in motion due to repeated contractions and expansions of the ruminal walls. The motion of the ruminal walls is tracked using depth sensitive

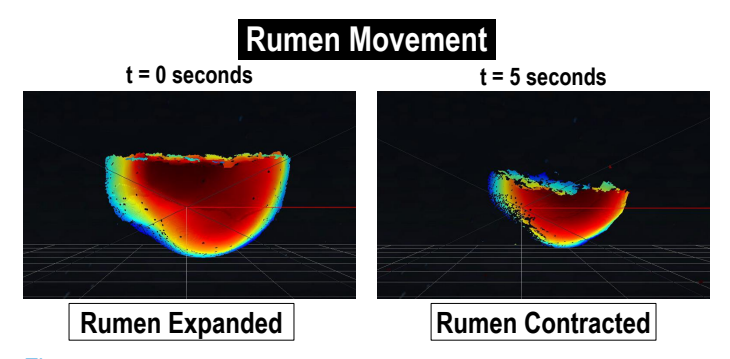


Fig. 5: The contraction of the rumen is captured using depth sensitive camera (Intel Realsense D435i) and is made available publicly on GitHub. The colors indicate distance from camera with red being the ruminal walls closer to camera and blue being walls further away.

Antenna Properties: Experiments

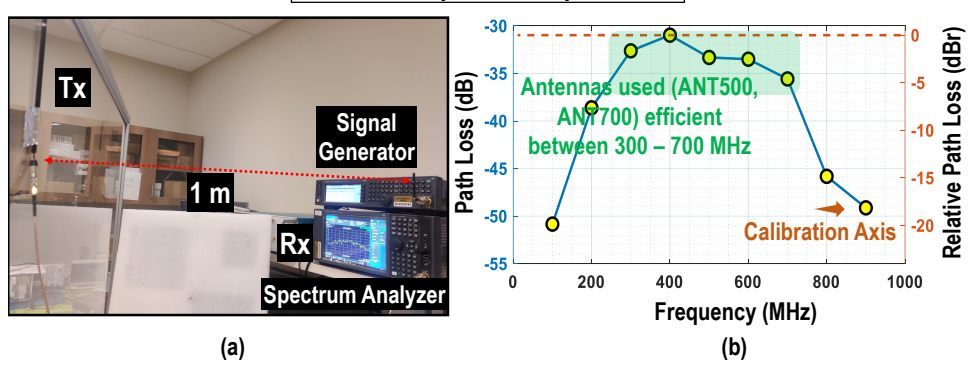


Fig. 6: (a) Setup to characterize the two antennas used in the experiments (ANT500 and ANT700) in free space. The two antennas are kept 1m apart and the signal is generated using a tabletop signal generator performing a frequency sweep while readings are taken on a tabletop spectrum analyzer. (b) The channel loss characteristics for the two antenna setup in free space is observed.

cameras (Intel RealSense D435i) and illustrated in Fig. 5. These images captured with depth sensitive cameras are color coded with red showing walls close to the camera and blue are the walls which are further away. The images show the movement of ruminal walls. Further, the contents inside the rumen are present in a stratified form with the top layer formed by gases, a middle layer formed by a dense mat of fibers and a bottom layer consisting of clear liquid [17], [18]. The transmitter is placed in between the dense mat of fibers in the middle layer. During the course of the experiments owing to the movement of the ruminal contents, the transmitter setup typically resides between the top and the middle layers of the rumen. As the whole setup is present floating inside the contents of the rumen, the movement of the ruminal walls makes the task of tracking the orientation of the transmitting antenna at any point in time difficult. Thus, the experiments contain a degree of uncertainty in terms of the position and the orientation of the transmitter setup. However, it is an extremely useful tool in providing channel loss ballpark values which are essential to verify the results obtained via simulations.

D. Experimental Results

The experimental results obtained for the frequency sweep conducted are described in the following text. The channel loss response is a function of the transceiver system used and we describe the frequency range for efficient communication using a particular system.

- 1) Antenna Properties: Fig. 6 illustrates the behavior of the two antennas ANT500 (transmitter) and ANT700 (receiver) in free space at a distance of 1 m, which is similar to the distance between transmitter and receiver during the in-body to out-of-body experiments described in the subsequent sections. The experiments are conducted in lab environment and the setup is shown in Fig. 6 (a) and the channel loss response in shown in Fig. 6 (b). The channel loss results illustrates that the two antennas are inefficient at frequencies below 300 MHz as well as frequencies above 700 MHz.
- 2) Data Calibration: The antenna properties are used to calibrate the path loss measurements taken via experiments in the dairy farm. The calibration is done by finding the frequency with the lowest path loss (400 MHz in Fig. 6 (b)) and fixing it to 0 dB in the calibration axis. The path loss in the other frequencies are found relative to the loss at 400 MHz. The relative path loss values as shown in the right hand Y axis of Fig. 6 (b) is subtracted from the experimental results (performed in the dairy farm, section III. D. 2 and 3) associated with their respective frequencies. This ensures that the effect of the specific properties of the antennas used in the experiments (ANT500 and ANT700) are mitigated from the experimental results.

3) Channel Loss Response vs Frequency: Channel Loss response as a function of frequency is illustrated in Fig. 7 (a). The results shown are for two specific receiver positions: position 8 on 1) collar and 2) opposite cannula as per Fig. 4. The path loss results obtained in Fig. 7 (a) are calibrated as described in Section III.D.1 and shown in Fig. 7 (b). This result illustrates the regions in which the In-Body to Out-of-Body animal body channel can be best used. We observe that the calibrated channel loss is low for frequencies above 500 MHz. An In-Body to Out-of-Body communication system for Bovines may use a frequency of operation in the range of 500 MHz

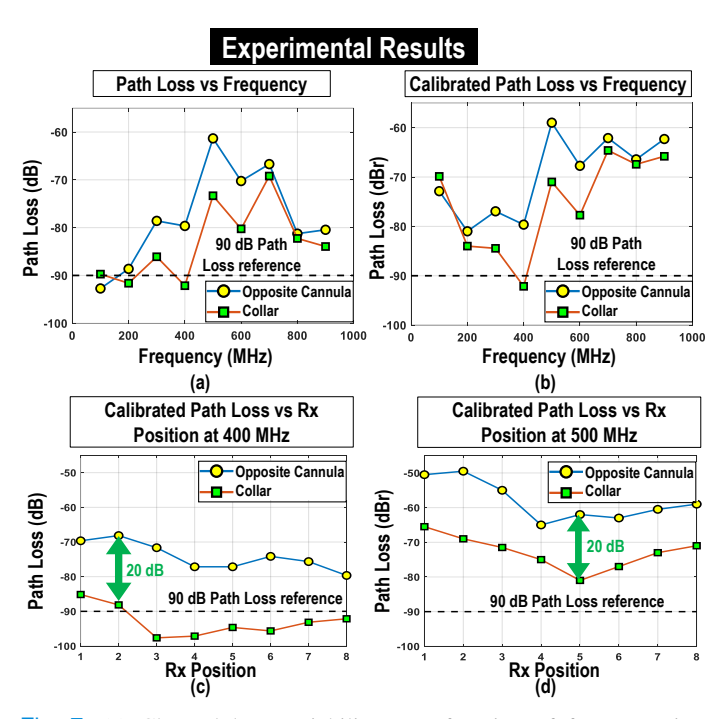


Fig. 7: (a) Channel loss variability as a function of frequency is illustrated. The receiver is placed in position 8 (Fig. 4) at both the locations, collar and opposite cannula. (b) The channel loss results in previous figure are calibrated using data from Fig. 6 (b) and the calibrated channel loss data for receiver in position 8 of collar and opposite cannula is presented. (c) Calibrated channel loss variability as a function of the receiver positions (Fig. 4) at a frequency of 400 MHz. The channel loss on the collar is more than the reference path loss of 90 dB. (c) Calibrated Channel loss characteristics as a function of position for an operating frequency of 500 MHz.

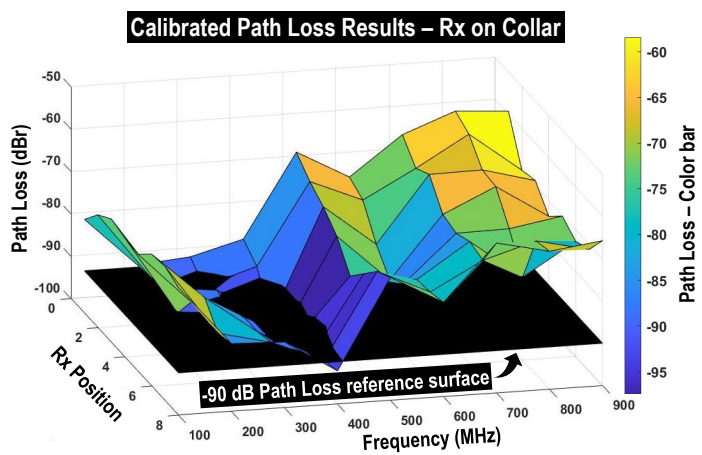


Fig. 8: Surface plot showing the channel loss response as a function of the receiver position and frequencies between 100 MHz to 900 MHz. The black surface marks the 90 dB reference used to compare the channel loss response observed with the maximum permissible loss for a typical commercial transceiver.

to 900 MHz for communicating data to the collar of the animal with relatively low channel loss. We further note that the channel loss at the collar for frequencies between 200 MHz and 400 MHz are close to or more than the reference path loss of 90 dB which makes it unsuitable for efficient communication from in-body to out-of-body for bovines with the current transmitter-receiver system.

4) Channel Loss Response vs Position of receiver: The calibrated channel loss results as a function of the position of receiver is illustrated in Fig. 7 (c) for 400 MHz and Fig. 7 (d) for 500 MHz. Comparing the two figures, it can be observed that the communication system is better suited to operate at 500 MHz offering a much lower channel loss than at 400 MHz. Further, we observe a high channel loss at the collar position of the receiver which crosses the reference path loss line of 90 dB. Typically, positions 4,5,6 show higher path loss than other positions due to the receiver being opposite to the position of the cannula and the signal path from transmitter to receiver through the body has the highest thickness of attenuating body tissues to cross. Further, channel loss is observed to be less for position 1 and 8 of the receiver due to their proximity to the transmitter thus having to cross lesser attenuating body tissues in its signal path.

E. Discussion: Variability in Experiments and Need for a Detailed 3D Model

The channel loss properties illustrated in Fig. 7 are a function of the morphological features of the body, the transmitter and receiver system used as well as the orientation of the antennas. In Fig. 8, a surface plot detailing the calibrated channel loss at different positions of the receiver on the collar across the sub-GHz frequency range is illustrated. The surface shown in black acts as the 90 dB channel loss reference used to judge the communication channel for a typical commercial transceiver. We observe that the channel loss in the low frequencies ($\leq 400 \text{ MHz}$) is high in general resulting in a channel loss close to 90 dB and the frequencies above 500 MHz providing lowest channel loss across the different positions. However, it is essential to also note that the controllability of parameters in the experiments is very low specifically in case of the transmitter which is inside the rumen. A change in the orientation of the transmitter due to ruminal contractions and expansions during the experiment will result in changing characteristics of the channel loss. As the transmitting device is not tethered to any point and is left to flow freely inside

the rumen, it is difficult to control or predict its exact position and orientation. There are two main methods to reduce the variation of channel loss due to changing position and orientation of the antenna. The first approach is to ensure that the transmitting antenna used has a very low directivity. Hence, an antenna which is as close to isotropic as possible radiating signal equally in all directions works best as the transmitter in this system. The signal radiated is not along any specific direction and maintains equal signal strength across all directions to ensure that changing orientation does not significantly change the signal strength in the direction of the receiver.

The second method to optimize receive signal strength despite the movement of the transmitter is by using adaptive transmit power control. Dynamic transmit power management in RF systems have been studied extensively [19], [20] and is used commercially in some applications. In our use case, a Channel Quality Indicator (CQI) can be calculated at the receiver end periodically and then fed back to the transmitter. The COI data received at the transmitter can inform the transmitter about the channel loss due to the current position and orientation of the transmitter. Using the CQI data, the transmitter adapts the output power to transmit at the lowest power needed to maintain signal integrity at the receiver end. The rumen contractions occur at regular intervals of about once a minute thus changing the position and orientation of the transmitter at the same rate. The adaptation time for a dynamic transmit power management system to change the transmit power is in the order of a few milliseconds. Thus, the transmitter can adapt its power at a much faster rate than the orientation of transmitter would typically change. This will enable the transmitter to increase or decrease the signal strength to have enough Signal to Noise ratio (SNR) to allow successful data communication, at the expense of higher power for bad orientations and provide power savings for good orientations.

The experimental results presented do a good job in providing a preliminary study for the channel loss responses. However, to have a reliable tool to get the ground truth for the communication channel we need to ensure parameters like transmitter orientation and positions are controllable. Thus, FEM simulations using the developed 3D

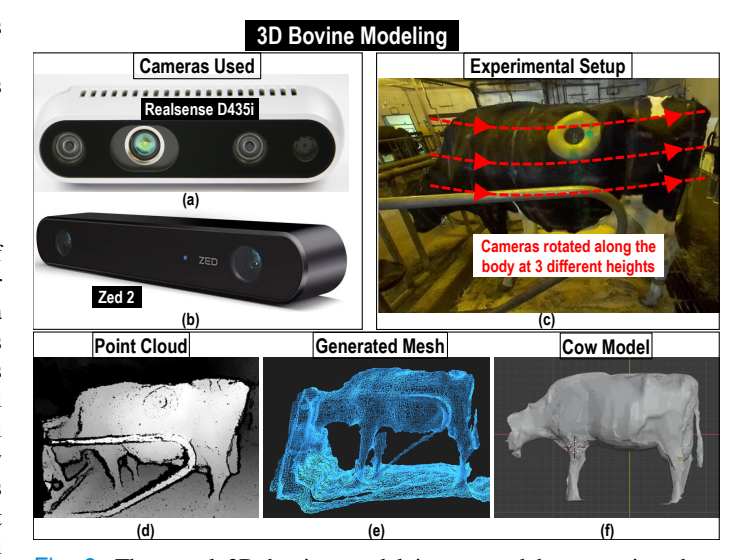


Fig. 9: The novel 3D bovine model is prepared by capturing the images using (a) Realsense D435i depth sensing camera, and (b) Zed 2 Stereo camera. (c) Images are captured by moving the camera across the body of the cow at different heights. (d) Point cloud generated by the images. (e) A mesh is created from the point cloud which is then used to create the solid model of the cow shown in (f).

bovine model allow us to capture the trends for all parameters being controllable. We use the experimental results as a baseline to judge the 3D bovine model's validity. An efficient simulation model allows us to capture the effects of all parameters separately thus providing the controllability that was lacking in the experimental results.

IV. 3D BOVINE MODELING AND FEM SIMULATION RESULTS

A. Need for a Simulation Model

Characterizing the signal propagation and signal strength from inside to outside the body demands a rich understanding of the physiology to precisely estimate the resistance posed by the many layers of body tissues. Bovines have an asymmetric distribution of organs, with the rumen on the left side and other vital organs such as the intestines and liver to the right. This asymmetry leads to varied signal attenuation around the body. With the transmitter placed inside the rumen, it becomes vital to characterize this distribution of signal strength around the animal body to identify key regions for receiver placement to achieve optimized communication. To understand and simulate the signal attenuation and link strength, a 3D model is built to be used for FEM based EM simulations of the animal.

The first step in building a rich model for simulations is creating a model of the body of the animal. Accuracy of the signal attenuation calculations depends upon the accurate characterization of the body contours and geometry. To this end, we first scan the body of the ruminant to build an exterior shell model that captures the body contours and scale, accurately.

B. Modeling Bovine Morphological Features

1) Experimental Setup: Building a 3D model of the animal's body is a non-trivial task as it requires mapping the contours of a continuous, irregular shape. Also, due to the size of the animal, it is difficult to precisely control the lighting during data collection. The animal also moves constantly which can result in blurry images and overlaps in depth data. The cow's coat is also a low-grade shiny surface which can result in specular refractions, thereby reducing the effectiveness of the infrared depth cameras. To overcome these hurdles, a set of RGB-D (Intel Realsense), Fig. 9 (a), and stereo (ZED Camera) cameras, Fig. 9 (b), are used in for the data capture. The RGB-D cameras and the stereo cameras are setup at strategic points on both sides of the animal as shown in Fig. 9 (c). The cameras were not setup to capture data from the front or the back of the cow as those points are of least interest for this application. Using carefully located tripods, data was collected at 3 different heights, 0.8m, 1.5m and 1.8m above ground level, to help gather enough data around the animal. The setup was assembled in the Purdue Dairy Farm and the recordings were conducted on an animal in a four-hour window to minimize the impact of daily variations in weight, water content, and environmental conditions.

2) Data Collection: Both Images and videos of the animal were captured using the RGB-D and stereo cameras. The images were taken at demarcated points, about 50cms from the animal to optimize for the precision in depth and the camera angle. The Realsense Viewer was used with with motion, depth, and RGB source enabled. Zed Explorer software was used with the Zed stereo camera and the images were taken at 1080p resolution. Videos were recorded of the animal, starting from the neck till the hind on both sides. The videos were captured primarily using the ZED camera due to its stereo capabilities and higher precision. A resolution of 1080p was used in this step. The height was varied for the videos with overlap in the view angle to facilitate stitching and model building in subsequent steps. The time stamped data was stored in a cloud-based server for

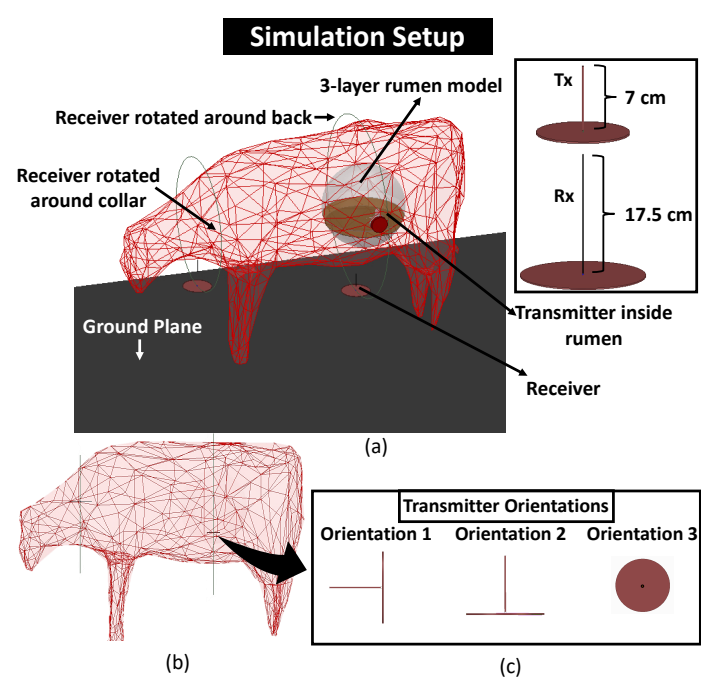


Fig. 10: (a) 3D bovine model used for FEM based EM simulations on Ansys HFSS solver. The bovine model accurately describes the structure of the bovine and a 3-layer rumen model is used to house the transmitter. The receiver is placed on the critical positions identified in Fig. 4. (b) The transmitter inside the rumen is placed in 3 orientations as described in the figure. This ensures that the movement of the transmitter inside the rumen is emulated.

further analysis. A total of 54 images and 12 videos were collected for this study.

3) Post Processing: After the initial processing, the images and videos needed to be post processed to build a 3D model which is the process of photogrammetry. The videos were processed using the ZED depth viewer to build baseline depth meshes of the animal's body. The software yielded clean meshes but it also captures the surroundings and losses due to camera angles resulted in loss of curvatures in key regions. Therefore, to supplement these meshes, meshes were generated from the point cloud data (Fig. 9 (d)) gathered using the RGB-D images. Using the Meshlab open-source software, the point clouds were cleaned for outliers and environmental areas were segmented. Occluding objects such as the grates and chains around the animal were also removed. The normal and curvatures were set in the Meshlab software with optimization to remove redundant density that hampers the calculations. A Poisson-disk sampling with Base Mesh subsampling and 5000 number of samples was used for this operation. These steps were repeated for all images and the generated results were saved in Polygon File Format (.ply) files. After initial cleaning and segmentation, the images were imported into a single file to fuse the point clouds together. Leveraging key identifier points in the outer anatomy such as the pelvic bones, the rib cage, the shoulder joints and the limb locations, the point clouds were scaled, aligned, and superimposed together. The ICP algorithm was used to glue the point clouds together. To generate a mesh from this set of point clouds, the surface reconstruction module of Meshlab was used with the parameter set to Poisson with an octree depth of 12. The mesh generated is illustrated in Fig. 9 (e). The resultant mesh was cleaned for protrusions and outliers. Finally, the mesh was superimposed with the video-generated meshes to correct for warping and holes in the models. The final

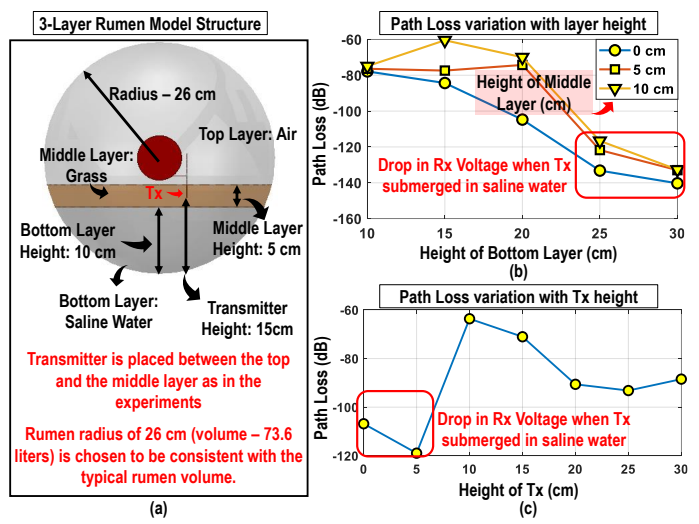


Fig. 11: (a) The structure of the rumen model developed is illustrated. The rumen consists of three layers, the top layer is filled with air, the middle layer emulates the feed and uses the material properties of grass and the bottom layer consists of saline water emulating ruminal fluids. (b) The variation in channel loss as a function of the height of middle and bottom layers is illustrated. The channel loss increases drastically when the transmitter is submerged inside the bottom layer. (c) The channel loss variability as a function of the height of transmitter is illustrated.

mesh was exported to Fusion 360 software to generate a surface model, as shown in Fig. 9 (f). Finally, using the depth measurements and published standard anatomic measurements for various layers of tissues and organs, a solid CAD model of the animal with a cavity for the rumen is built. This model was exported to the HFSS software for further modeling and simulation.

C. FEM Simulation Setup

The 3D model created is used for Finite Element Method based EM simulations using Ansys High Frequency Structure Simulator (HFSS) as shown in Fig. 10 (a). The simulations are run at a frequency range of 100 MHz to 900 MHz similar to the experiments. The 3-layer spherical space is used to emulate the rumen which houses the transmitter. The rumen leads to an opening on one side of the cow model's body which is closed with a hard rubber cylindrical structure as per the cannular region in the experimental setup shown in Fig. 3 (d). The body of the 3D model consists of muscle layer [21] which is the predominant tissue in the body and thus efficiently models the attenuating effect that the body has on the signals. Similar FEM based EM studies using simplified simulation structures have previously been conducted to perform channel modeling on human bodies [22]–[25] with a high degree of accuracy. The transmitting and receiving antennas are modelled after the setup that were used in the experiments. Thus, the receiver is designed as a monopole antenna of the same length as the telescopic antenna (ANT500) used with no extension and the transmitter is a monopole antenna of the same length as the telescopic antenna (ANT700) at no extension as illustrated in Fig. 10 (a). Lumped port excitation with a full port impedance of 50 Ω is used as the excitation for the setup. Once the transmitter is placed inside the rumen of the cow's body in the experiments, the transmitter moves due to the constant movement of the rumen walls thus changing orientation during the course of the experiments. To show the effect of changing orientations, we place the transmitter antenna inside the rumen in 3 different orientations

as shown in Fig. 10 (b). The transmitter orientations chosen in this study is not an exhaustive list, but the effect of orientations can be effectively portrayed with the 3 orientations shown. The receivers are rotated on the opposite side to the side of the body where the cannula is present similar to the experimental case. The receivers are rotated along 8 points on two positions (Fig. 4): 1) around the collar, 2) around the body opposite to cannula as per the experiments conducted.

D. Rumen Modeling

The ruminal contents are present in a stratified form as illustrated in the model in Fig. 11 (a) [17]. A 3 layered rumen structure where the top layer material is air, the middle layer material is modelled as grass emulating the feed for the cow and the bottom layer consists of saline water emulating the fluids inside the rumen is used. The rumen is a spherical structure with a radius of 26cm for a volume of about 73.6 liters which is similar to typical ruminal volume [26]. This has been illustrated in Fig. 11 (a).

The variation in thickness of these layers changes the channel loss characteristics as illustrated in Fig. 11 (b). For this simulation, the transmitter is kept at a fixed position around the center of the rumen in orientation 1. The results are shown with the receiver fixed at position 8 on the body of the cow opposite to the cannula. The simulation is performed at a frequency of 400 MHz. The figure shows the variation of path loss with changing height of the bottom layer (saline water) for 3 different heights of the middle layer (grass) with the transmitter fixed at a position in the center of the rumen. Note, that varying the height of the middle layer and bottom layer also changes the height of the top layer as the spherical rumen structure remains the same. We observe that the path loss drastically increases when the transmitter is submerged inside the bottom layer (saline water) which being a conductor adds additional losses. We also observe that the increasing height of middle layer (grass) helps the signal strength.

The variation of channel length with changing transmitter height along the rumen is illustrated in Fig. 11 (c). The same setup is used with the receiver fixed at position 8 on the body opposite to the cannula and the simulation performed at 400 MHz. When the transmitter is submerged inside the bottom layer (saline water) for a transmitter height of less than 10 cm, the channel loss is above 100dB. When the transmitter is submerged in the ruminal content or in air, the channel loss decreases. We observe that the loss is less when the transmitter is submerged in the middle layer compared to when it is completely in the top layer (air). Thus, the transmitter must be either left floating on top of the middle layer or between the top layer (air) and the middle layer to ensure lower path loss. Using this knowledge, for the subsequent simulations we fix the middle

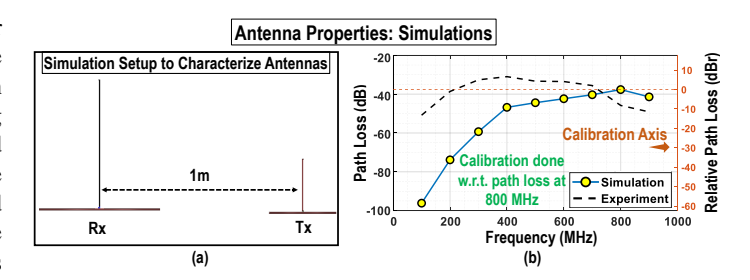


Fig. 12: (a) The antenna used in the simulations are designed to be structurally similar to antennas used in experiments. The setup used to characterize the antenna in free space for the simulation environment used is illustrated. (b) The channel loss for the two antennas (transmitter and receiver) are compared with the antenna characteristics for the pair of antennas used in the experiments.

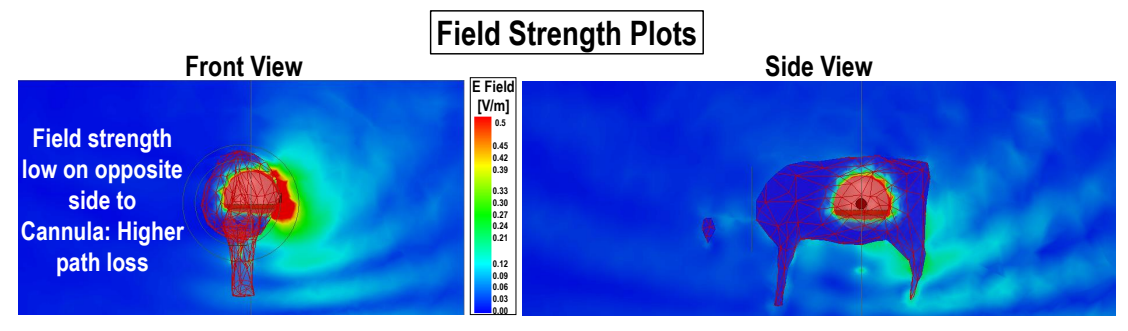


Fig. 13: Field strength plots using Ansys HFSS for an operating frequency of 500 MHz is illustrated. The field plots show the rapid decay in field strength inside the body of the cow due to the presence of attenuating body tissues. We also observe reduced field strength on the opposite side of the cannula. Increasing the accuracy of the simulations using finer meshing will allow for more precise field strength plots with uniform field distribution. However, the baseline trends observed will be the same as illustrated in this figure.

layer height to 5 cm and the bottom layer height to 10 cm with the transmitter at a height of 15 cm which places it between the top and the middle layers of the rumen. This condition is similar to the experimental setup where the transmitter is placed between the air layer and the feed in the rumen.

E. Simulation Results: Validating the Bovine Model Developed

1) Antenna Design and their Behavior at sub-GHz Frequencies: The antennas are designed to be similar structurally and are of the same length to the antennas (ANT500, ANT700 when they are folded back completely) used in the experiments (Fig. 3 (a)). However, the antenna properties are not an exact match to the antennas used in experiments. The two telescopic antennas used in the experiments are designed to operate in a broad frequency range efficiently as illustrated in Fig. 6. Further, multipath effects and other second order effects modify the channel loss in a lab or dairy farm environment for the antennas. Fig. 12 (a) shows the setup to measure the channel loss of the antenna pair in free space. Fig. 12 (b) illustrates the path loss between the transmitter and receiver used in free space with air medium in between with a separation of 1 m between the two antennas as done previously in the experiments (Fig. 6 (a)). The results have been shown in comparison to the antenna properties in case of the experiments as illustrated in Fig. 6 (b). The antennas used in simulations are efficient at frequencies beyond 400 MHz similar to the experimental antennas. However, the channel loss rolls off drastically for frequencies less than 400 MHz and this high path loss will also be evident in the uncalibrated simulation results (Fig. 14 (a) and (c), Fig. 15(a) and (c)).

2) Calibration of Simulation Results: To mitigate the effects of the antenna properties affecting the channel loss results, we calibrate the results from the in-vivo simulations. For calibration, we use a similar process as performed in the experiments. The channel loss in free space for a separation of 1 m between transmitter and receiver (Fig. 12 (b)) is analyzed to find which frequency provides the lowest channel loss (800 MHz in this case). The channel loss for other frequencies are calculated relative to the channel loss for 800 MHz. The relative channel loss values (dBr values) are subtracted from the channel loss results for respective frequencies in the in-vivo In-Body to Out-of-Body (IBOB) simulations. This process allows us to reduce the affects of the antenna properties used in simulations and allows an unbiased view of the channel for sub-GHz frequencies.

F. Path Loss vs Frequency

The effect of attenuating body tissues is illustrated at 500 MHz with the field plots shown in Fig. 13 (a) and (b) from the front and side view respectively. The figure shows that the field strength decays rapidly when passing through the body. We also observe that the field strength decay in air is much more gradual as compared to that inside

the body. Further, from Fig. 13, we observe that the field strength on the side of the cannula is much higher than that on the opposite side to where the cannula is present.

Fig. 14 (a) and (c) show the variation of channel loss with frequency for the two cases of the receivers positioning. The corresponding calibrated path loss values vs frequency is illustrated in Fig. 14 (b) and (d) for receiver on body and collar respectively. The receiver is fixed at position 8 for both positions: collar and on the body opposite to cannula (Fig. 4). The channel loss results are shown for 3 different orientations of the transmitter as described in Fig. 10 (b) and the difference in trends due to changing orientation of the transmitter is presented. The calibrated channel loss results show that for the receiver placed opposite to the cannula, the channel loss across all frequencies is less than the reference path loss of

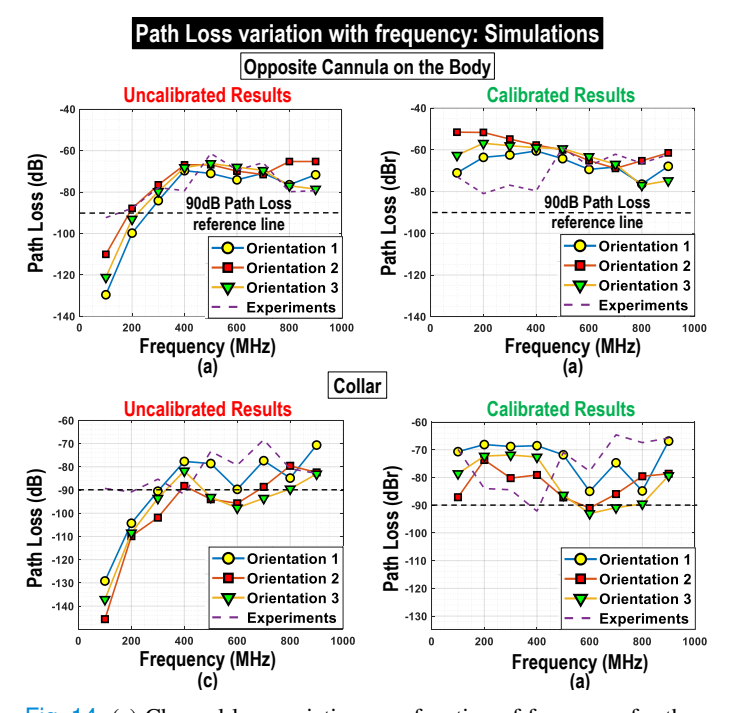


Fig. 14: (a) Channel loss variation as a function of frequency for the three orientations of the transmitter inside the rumen is illustrated for the receiver on the body of the cow opposite to the cannula at position 8. (b) Calibrated channel loss results vs frequency for receiver on the body opposite the cannula in position 8. (c) Channel loss variation as a function of frequency with the receiver on the collar of the cow at position 8. (d) Calibrated channel loss results as a function of frequency for the receiver on the collar of the cow at position 8.

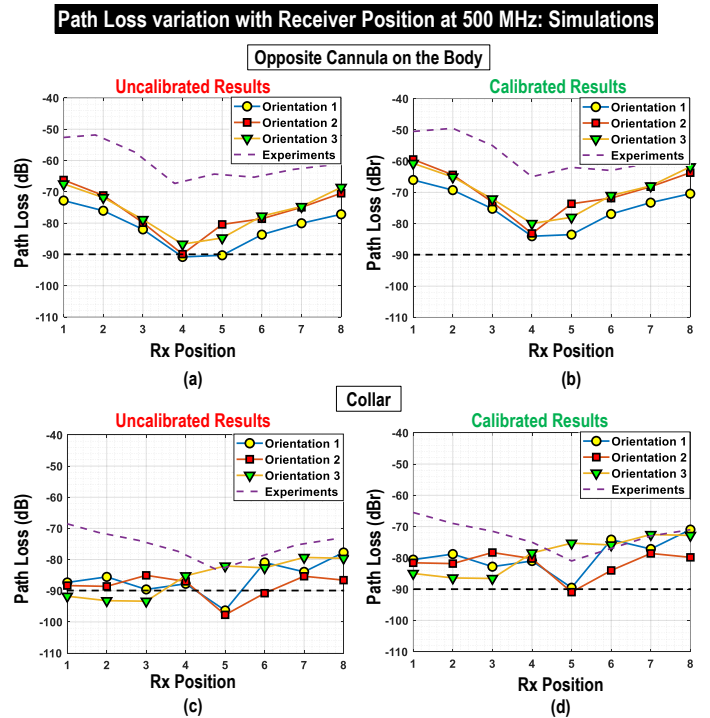


Fig. 15: (a) Channel loss variation with respect to position of the receiver as per Fig. 4 is shown for an operating frequency of 500 MHz for the receiver moving around the body opposite to the cannula. (b) Calibrated results for the data shown in figure (a). (c) Channel loss results with respect to the position of receiver moving around the collar at 500 MHz. (d) Calibrated channel loss results with respect to the position of the receiver around the collar at 500 MHz.

90dB that we considered can be handled by a commercial transceiver (Section III. A.). However, when the receiver is moved around the collar of the cow, the channel length and corresponding channel loss increases. We observe that the calibrated path loss (Fig. 14 (d)) may be greater than 90dB depending upon the orientation of the transmitter. We observe a comparatively lower channel loss for frequencies below 500 MHz and at 900 MHz. The channel loss is close to 90 dB across all frequencies between frequencies 500 MHz to 800 MHz when the receiver is placed on the collar. However in the experiments, the channel loss at frequencies above 500 MHz were lower than the channel loss at other frequencies as shown in Fig. 7. This variation in experiment and simulation results are due to the changes in experimental conditions and more strongly due to transmitter orientation and position variations during the course of the experiments. The simulations provide us a method of isolating the effects of positional variance in transmitter and the frequency sweep performed (Fig. 14) shows the frequency regions (100 - 400 MHz) where best to operate for lower channel loss of the system.

G. Path Loss vs Position of receiver

The variation of path loss with the changing position of the receiver along the body of the cow opposite to the cannula as well as along the collar is shown in Fig. 15 (a) and (c) respectively. The raw data is then calibrated and presented in Fig. 15(b) and (d) for receiver along the body opposite to cannula and receiver on the collar respectively. The simulations are performed for the three orientations of the transmitter at an operating frequency of 500 MHz. The trends due to positional variance in path loss are similar in experiments and simulations. We observe that the channel loss is lower for positions 1 and 8 for both experiments and simulations. Further, position 5 shows higher path loss in general than other positions as it is directly opposite to the

cannula and thus, the channel between transmitter and receiver has to pass through higher number of body tissues thus having a higher attenuation. Channel loss being less for receiver positions 6,7,8 on the collar (Fig. 15 (d)) on the simulations as well as in the experiments is an important conclusion as position 6,7,8 on the collar are the typical positions of bells below the collar where a receiving device can be expected to hang in most situations.

V. Novel 3D Model for IBOB Communication in Animals and Future Work

A. 3D Bovine Model

The simulations performed above illustrate that the 3D model developed for FEM based EM studies on bovines is an accurate and efficient tool for channel modeling at various sub-GHz frequencies. The studies conducted here show that the channel loss results follow similar trends to those observed in experimental studies and that the path loss can be accurately measured with the use of such a model for changing position of transmitter and receiver. The 3D bovine model developed allows controllability in tweaking the parameters involved in the experimental setup to observe the channel loss trends. From the study performed, we can isolate the effect of channel loss variation due to the changing orientation and position of the transmitter and receiver. The experimental studies performed provide us with baseline trends and channel loss results which are used to validate the performance of the bovine model. The channel loss response is seen to be a function of the characteristics of the transmitter and receiver setup used. To mitigate the effects of the transmitter and receiver setup, a calibration was performed to remove the bias of the transceiver characteristics on the channel models. The novel bovine model developed provides a complete simulation environment accurately modeling the morphological features unlike previous multi-layered tissue structures, and thus closely follows the experimental trends observed. The model can be used to test other communication systems with different transmitter-receiver pairs to analyze the performance at different frequencies and to figure out the best operation point for communicating signals from in-body to out-of-body in bovines. The approach of using computer vision techniques to model the morphological features of the animal body and use the developed 3D model of the body can be used in scenarios not pertaining to dairy animals as well for accurate communication channel modeling.

B. Channel Loss Optimization for Animal IBOB Communication

As previously described in Section III. C, the orientation and position of the transmitter can not be fixed for a device that is floating inside the rumen. Thus, an isotropic antenna should be used to ensure that the effect on channel loss due to changing orientation and position of the transmitter is minimized. This ensures that the transmitter radiates in all directions reducing the effect of changing orientation. Another method to efficiently radiate signal in multiple directions is to introduce multiple small antennas directed in different directions and intelligently choosing which antenna to transmit data to reduce channel loss. This approach may be further enhanced to use phased array antennas where an array of small antennas transmit at different phases to change the direction in which the whole setup radiates dynamically. These methods along with adaptive transmit power control (Section III. E) can be employed to optimize channel loss for In-Body to Out-of-Body communication in ruminants.

C. Future Work

Subsequent work based on this channel modeling would focus on the development of a resource constrained low power integrated system with sensing and communication capabilities. The novel experimental technique and open-source 3D Bovine model developed also enables further research on in-farm networks with increased scope capturing more data points of channel loss on and around the body of the cow leading to statistical modeling for In-Body to Out-of-Body Communication in dairy farm setup. Further, the use of this novel channel modeling method will also pave the way for future studies analyzing in-body to out-of-body communication channels for other animals in the smart animal agriculture space.

VI. CONCLUSION

We present a novel channel modeling methodology for in-body to out-of-body animal body communication which provides a framework to develop an efficient communication system for the first hop of a farm network. The results demonstrate that an in-body to out-of-body communication from the rumen to the collar of a ruminant is possible with $\leq 90dB$ path loss across sub-GHz frequencies (100 - 900MHz). The channel model developed allows us to exploit the path loss characteristics of the animal in-body to out-of-body communication channel to come up with an operating frequency that provides the lowest path loss thus ensuring low power communication. This is essential for in-body to out-of-body communication design due to the nature of the transmitter node which is inside the body of the animal will be size constrained and thus have a small battery. A low power communication methodology will thus extend the battery life of such a device. The channel model is validated using novel experimental methods on a cannulated cow which provides direct access to the rumen. The transmitter is housed inside the rumen and the receiver is moved along critical positions on the body of the cow. The results are used to validate a first-of-its-kind open-source 3D bovine model made publicly available on GitHub [4]. The model was developed using computer vision techniques for finite element method based electromagnetic simulations performed on Ansys HFSS. This method of creating a channel model can be replicated for other similar animal in-body to out-of-body communication channels thus paving the path for further studies on communicating data efficiently from sensors dwelling inside the animal body to a node on the body.

ACKNOWLEDGEMENTS

This authors wish to acknowledge the support of USDA, through the NRI and CPS programs, under grants 2018-67007-28439 and 2019-67021-28990 and the National Science Foundation Career Award under Grant CCSS 1944602. Opinions represent those of the authors and not the agency. A. Datta, M. Nath, B. Chatterjee and S. Sen are with the Elmore Family School of Electrical and Computer Engineering, U. Kaur and R.M. Voyles are with School of Engineering Technology at Purdue University, West Lafayette, IN 47907 USA. V. Malacco is with MSU Extension at Michigan State University, East Lansing, MI USA. S. Donkin is with College of Agricultural Sciences at Oregon State University, Corvallis, OR 97331 USA. Corresponding author: Shreyas Sen, e-mail: shreyas@purdue.edu

REFERENCES

- S. Sen, S. Maity, and D. Das, "The body is the network: To safeguard sensitive data, turn flesh and tissue into a secure wireless channel," *IEEE Spectrum*, vol. 57, no. 12, pp. 44–49, 2020.
- [2] S. Sriram, S. Avlani, M. P. Ward, and S. Sen, "Electro-Quasistatic Animal Body Communication for untethered rodent biopotential recording," *Scientific Reports*, vol. 11, no. 1, pp. 1–14, 2021.
- [3] D. Das et al., "Enabling Covert Body Area Network using Electro-Quasistatic Human Body Communication," Scientific Reports, vol. 9, no. 1, Mar 2019. [Online]. Available: http://par.nsf.gov/biblio/ 10153369
- [4] Sparclab. (2021) 3D Bovine FEM Model. [Online]. Available: https://github.com/SparcLab/Bovine-FEM-Model.git

- [5] Federal Communications Commission. (1999)
 MedRadio. [Online]. Available: https://www.fcc.gov/medical-device-radiocommunications-service-medradio
- [6] LoRa Alliance. LoRa. [Online]. Available: https://lora-alliance.org/
- [7] Connectivity Standards Alliance. ZigBee. [Online]. Available: https://csa-iot.org/all-solutions/zigbee/
- [8] A. Datta, M. Nath, B. Chatterjee, N. Modak, and S. Sen, "Channel Modeling for Physically Secure Electro-Quasistatic In-Body to Out-of-Body Communication with Galvanic Tx and Multimodal Rx," in 2021 IEEE MTT-S International Microwave Symposium (IMS). IEEE, 2021, pp. 116–119.
- [9] "NEVA Electromagnetics LLC | VHP-Female model v2.2 VHP-Female College," https://www.nevaelectromagnetics.com/vhp-female-2-2, [accessed August 27, 2020].
- [10] H. Dogan et al., "UHF wave attenuation throughout the cow body," in 2017 10th International Conference on Electrical and Electronics Engineering (ELECO). IEEE, 2017, pp. 1046–1049.
- [11] H. Dogan, I. B. Basyigit *et al.*, "Signal level performance variation of radio frequency identification tags used in cow body," *International Journal of RF and Microwave Computer-Aided Engineering*, vol. 29, no. 7, p. e21674, 2019.
- [12] R. Kronberger et al., "Animal body model to improve the development of UHF RFID transponders for animal detection," in 2019 IEEE International Conference on RFID Technology and Applications (RFID-TA). IEEE, 2019, pp. 224–226.
- [13] D. Gottardi et al., "Animal skin phantom for RFID UHF transponder development," in 2018 International Symposium on Antennas and Propagation (ISAP). IEEE, 2018, pp. 1–2.
- [14] A. Datta, U. Kaur, V. Malacco, M. Nath, B. Chatterjee, S. S. Donkin, R. M. Voyles, and S. Sen, "In-body to Out-of-body Communication Channel Modeling for Ruminant Animals for Smart Animal Agriculture," in 2021 43rd Annual International Conference of the IEEE Engineering in Medicine & Biology Society (EMBC). IEEE, 2021, pp. 7570–7573.
- [15] Great Scott Gadgets . (2021) ANT700. [Online]. Available: https://greatscottgadgets.com/ant700/
- [16] A. Rahman, D. Smith, B. Little, A. Ingham, P. Greenwood, and G. Bishop-Hurley, "Cattle behaviour classification from collar, halter, and ear tag sensors," *Information Processing in Agriculture*, vol. 5, no. 1, pp. 124–133, 2018. [Online]. Available: https://www.sciencedirect.com/science/article/pii/S2214317317301099
- [17] P. Smith, H. Sweeney, J. Rooney, K. King, and W. Moore, "Stratifications and kinetic changes in the ingesta of the bovine rumen," *Journal of Dairy Science*, vol. 39, no. 5, pp. 598–609, 1956. [Online]. Available: https://www.sciencedirect.com/science/article/pii/S0022030256947919
- [18] U. Kaur, R. M. Voyles, and S. Donkin, Future of animal welfare technological innovations for individualized animal care. Wallingford, UK: CABI, 2021, no. Ed.3, pp. 351–362.
- [19] S. Sen, R. Senguttuvan, and A. Chatterjee, "Environment-adaptive concurrent companding and bias control for efficient power-amplifier operation," *IEEE Transactions on Circuits and Systems I: Regular Papers*, vol. 58, no. 3, pp. 607–618, 2010.
- [20] Cisco. Transmit Power Control (TPC) and Dynamic Frequency Selection. [Online]. Available: https: //www.cisco.com/c/en/us/support/docs/wireless-mobility/80211/ 200069-Overview-on-802-11h-Transmit-Power-Cont.html
- [21] S. Gabriel et al., "The dielectric properties of biological tissues: II. measurements in the frequency range 10 Hz to 20 GHz," *Physics in Medicine and Biology*, vol. 41, no. 11, pp. 2251–2269, nov 1996.
- [22] S. Maity, M. He, M. Nath, D. Das, B. Chatterjee, and S. Sen, "Bio-physical modeling, characterization, and optimization of Electro-Quasistatic Human Body Communication," *IEEE Transactions* on *Biomedical Engineering*, vol. 66, no. 6, pp. 1791–1802, 2018.
- [23] S. Maity et al., "On the safety of Human Body Communication," *IEEE Transactions on Biomedical Engineering*, pp. 1–1, 2020.
- [24] N. Modak, M. Nath, B. Chatterjee, S. Maity, and S. Sen, "Bio-physical modeling of Galvanic Human Body Communication in Electro-Quasistatic regime," bioRxiv, 2020.
- [25] A. Datta et al., "Channel modeling for physically secure Electro-Quasistatic In-Body to Out-of-Body Communication with Galvanic Tx and Multimodal Rx," in (presented) 2021 IEEE MTT International Microwave Symposium (IMS). IEEE-MTT, 2021.
- [26] J. Russell, "Rumen," in Encyclopedia of Microbiology (Third Edition), third edition ed., M. Schaechter, Ed. Oxford: Academic Press, 2009, pp. 163–174. [Online]. Available: https://www.sciencedirect.com/ science/article/pii/B9780123739445000614